Materials Science & Engineering A 612 (2014) 46–53

Contents lists available at ScienceDirect

Materials Science & Engineering A

journal homepage: www.elsevier.com/locate/msea

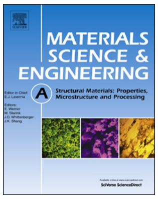

Designing quadplex (four-phase) microstructures in an ultrahigh carbon steel

H. Zhang*, D. Ponge, D. Raabe*

Max-Planck Institut für Eisenforschung, Max-Planck Str 1, 40237 Düsseldorf, Germany

ARTICLE INFO

Article history:
Received 22 May 2014
Received in revised form
5 June 2014
Accepted 9 June 2014
Available online 17 June 2014

Keywords:
Steel
Quadplex microstructure
Thermomechanical processing
Strain
Electron backscatter diffraction (EBSD)

ABSTRACT

Here we present an approach to design a ferrite-based quadplex microstructure (ferrite/martensite/carbide/austenite) using a lean alloyed Mn–Si–Cr–Al ultrahigh carbon steel. The material has 1500 MPa tensile strength and 11% elongation. The thermomechanical processing includes two main steps, namely, first, the formation of a ferrite plus carbide duplex microstructure by warm rolling below Ae_1; and second, annealing just above Ae_1 for a short time (~20 min). The quadplex microstructure consists of 57 vol% ultrafine ferrite (mean grain size ~1.5 μm), 29 vol% martensite, 12 vol% spherical carbide and 2 vol% austenite. Fracture analysis after tensile deformation reveals a mixed ductile and brittle failure mode without necking. Scanning electron microscopy (SEM), electron backscatter diffraction (EBSD) and dilatometry tests were conducted to map the microstructure characteristics and the contribution of each phase to the overall deformation.

1. Introduction

There is a high demand for steels with both, high strength and good ductility. Ultrafine-grained dual- or multiphase steels are of high interest in that context due to their potential to meet this demand: Ultrafine grain structures of such multiphase steels are enhancing strength and toughness through the interaction between the different phases [1,2].

However, single phase ultrafine-grained alloys, particularly those with nanometer-sized grains, show a high tendency for early necking due to their limited strain hardening rate [3–11]. Therefore, structural alloy design should not focus on extreme grain refinement alone, but also on improved ductility in multiphase systems where optimization of the phase fractions, their micromechanical interactions and their individual mechanical properties is essential.

The combination of both effects, i.e. grain refinement and the use of two phases has been realized in ultrafine-grained ferrite/martensite dual-phase steels [12–18]. They are attractive for lightweight constructions because they combine high tensile strength and good formability. In recent years, ferrite grains have been refined to submicron/micron class using severe plastic deformation combined with annealing [18] and thermomechanical processing [12,13,19] in ferrite/martensite dual-phase steels. Emphasis was placed on the effect of ferrite grain size on mechanical properties. Due to lean alloying and the associated effects on the individual phase properties, the obtained mechanical properties (tensile strength of 1000 MPa and 15% elongation [18]) are still subject to further improvement. Therefore, novel design ideas for ferrite/martensite dual-phase steels that are not based on ferrite grain refinement alone are required. Besides the grain size influence, the volume fraction, morphology and distribution of martensite strongly affect the mechanical properties of ferrite/martensite dual-phase steels [20–22]. In ferrite/martensite dual-phase steels, ferrite (soft phase) and martensite (hard phase) undergo a complex stress- and deformation partitioning when subjected to loading. The necking and fracture processes are delayed to large strains due to continuous work hardening determined by the heterogeneous distribution of dislocations [23]. Essentially, local hardening of ferrite occurs in the vicinity of martensite, which is caused by geometrically necessary dislocations (GNDs) [24].

In approaches to extent this composite concept from two to three interacting phases, "triplex" steels with carbide-free bainite/martensite/austenite [25] or martensite/austenite/k´-carbide microstructures [26–28] have been reported to exhibit an excellent strength–ductility balance. Some of the observed strengthening mechanisms have been associated with solid solution, carbide strengthening, and TPIP as well as TWIP effects. Also, the increase in the overall interface density induced by the additional phases could also improve mechanical properties [28].

These examples all imply a latent principle that a mixture of soft and hard phases in materials could realize a good combination of

---

* Corresponding authors.
E-mail addresses: h.zhang@mpie.de (H. Zhang), d.raabe@mpie.de (D. Raabe).

http://dx.doi.org/10.1016/j.msea.2014.06.023
0921-5093/© 2014 Elsevier B.V. All rights reserved.

strength and ductility via optimal stress/strain partitioning. Therefore, we present here the idea of designing a more complex multiphase system, i.e. quadplex (four phase) microstructures, trace their property response and shed light on future option for the individual phase design. In order to elucidate the property potential associated with such quadplex microstructures, we select here a lean low-alloyed ultrahigh carbon steel as a model material [29]. Essentially, the ultrahigh carbon content is not a necessity for such phase design and could be reduced at a later design stage to facilitate welding.

2. Experimental

A steel with composition 1.3C–2.3Mn–1.7Si–1.1Cr–1.0Al (wt%) was used. Mn improves hardenability. Mn and C are both favorable for obtaining some retained austenite and contribute to solid solution strengthening. Si and Al stabilize ferrite and suppress the formation of network carbides [30]. Cr stabilizes the carbides and retards their coarsening at high temperatures [31].

The alloy was produced by vacuum induction melting and cast in 70 mm × 70 mm billets. The thermomechanical processing diagram is shown in Fig. 1 (Ae_1 and A_{cm} measured by a Bähr Dil805 A/D quenching and deformation dilatometer). As indicated, ferrite plus carbide duplex microstructure (abbreviated by DP), ferrite-based and martensite-based quadplex microstructures (abbreviated by FQP and MQP) were obtained. Dog bone-shaped flat tensile specimens were machined from the plates after thermomechanical processing and used for tensile testing on an Instron 8800 tensile machine at 293 K and a strain rate of $10^{-3}\,s^{-1}$. The crosshead displacement was measured by a displacement sensor. In order to obtain the exact elongation of the tensile specimens, the gauge length (gauge length: 13.8 mm) was marked and measured again after the test. For each microstructure state, five tensile specimens were probed. Microstructure characterization and fracture analysis were conducted using a JEOL-6500F high-resolution field-emission scanning electron microscope operated at 15 kV. EBSD data (step size 100 nm) were analyzed with the TSL OIM 6.2 analysis software (combined with ImageJ software [32]) for grain size and phase fractions. As a qualitative measure for the defect content of the crystals [33,34], the image quality (IQ) of the EBSD maps was used to distinguish martensite and ferrite [35,36]. The martensitic regions with a high defect density have a low IQ value (dark zone) [37]. For mapping the local orientation gradients inside the bcc matrix (i.e. ferrite and martensite), the kernel average misorientation (KAM) values were calculated within the first nearest neighbor shell with a maximum misorientation angle of 2°. Generally, a high KAM value corresponds to a high dislocation density [38,39]. Dilatometer tests were performed with ∅ 4 × 9 mm^2 cylindrical specimens to measure the martensite start temperature (M_s) during quenching. The reference specimens with DP microstructure were heated at 10 K/s to 1053 K, isothermally held for a period of time (5 min, 20 min, 40 min, 60 min, 120 min and 180 min) and then cooled down to 293 K at 50 K/s. The isothermal holding for 20 min and 60 min correspond to the final step in the thermomechanical processing routes for obtaining FQP and MQP microstructures, respectively.

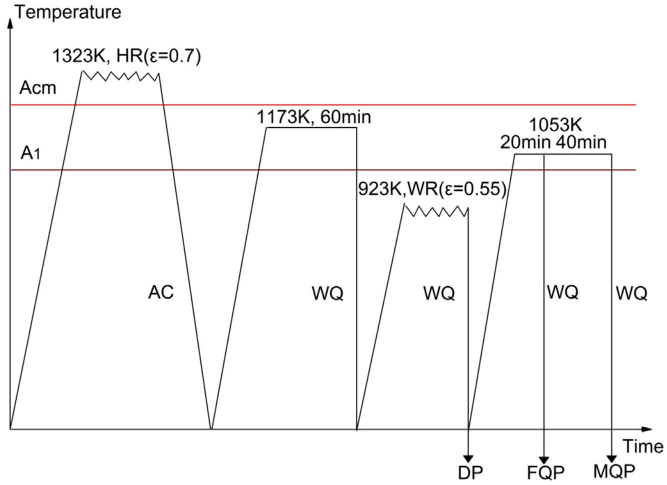

Fig. 1. Thermomechanical processing routes to produce different microstructures (DP: ferrite plus carbide duplex microstructure; FQP: ferrite-based quadplex microstructure; MQP: martensite-based quadplex microstructure; HR: hot rolling; WR: warm rolling; AC: air cooling; WQ: water quenching).

3. Results

3.1. Initial microstructures

Fig. 2a–c shows the phase plus IQ EBSD maps of the DP, FQP and MQP microstructures. The average grain size and phase fractions are listed in Table 1. The DP microstructure is composed of ferrite and spherical carbides while the FQP and MQP variants contain martensite and austenite apart from ferrite and carbide. The average grain size of ferrite and carbides (as well as the volume fraction of carbides) are similar among these microstructures. However, the volume fractions of ferrite, martensite and austenite show obvious differences, which can be also revealed by the secondary electron (SE) images in Fig. 2d–f. A high dispersion of nanometer/submicron-sized carbides (e.g. within the red circle in Fig. 2d) are observed in the DP microstructure. This feature is different from the FQP and MQP microstructures as indicated in Fig. 2e and f. Compared to Fig. 2f, the martensite blocks in Fig. 2e seem to be finer. Fig. 3 reveals the martensite start (M_s) temperatures during cooling after isothermal annealing at 1053 K with the initial DP microstructure (FQP and MQP microstructures obtained after annealing for 20 min and 60 min, as marked by the green and red circles). The M_s temperature drops with decreasing annealing time. For the case of isothermal annealing for 5 min, martensite transformation during cooling is not detected. This indicates that a short annealing period of 5 min at 1053 K is not sufficient for austenite formation.

3.2. Tensile testing

Fig. 4a shows the tensile curves of the DP, FQP and MQP specimens. The continuous increase of the engineering stress indicates that necking is prevented in all cases. The inlet of the fractured FQP specimen reveals uniform deformation. Compared to the DP variant with a yield plateau, the strain hardening rate of the FQP and MQP specimens is relatively high throughout tensile testing, as indicated by Fig. 4b. Table 2 summarizes the mechanical properties of these specimens. The FQP specimen exhibits the optimum combination of strength and ductility (UTS: ~1500 MPa; UE: ~11%).

3.3. Microstructures near fracture zones after tensile testing

Fig. 5a and b reveals the phase plus IQ EBSD maps of the FQP and MQP microstructures near the fracture zones after tensile testing. Compared to those prior to tensile testing (Fig. 2b and c), they do not show much difference except that austenite is hardly observed after deformation. The average KAM value of the bcc phase (ferrite plus martensite) in the ferrite-based FQP material increases greatly from the initial state where it had an average value of 0.45° to value of 0.84° after ~11% strain (Fig. 5c). For the martensite-based MQP, the average KAM value of bcc phase increases marginally from 0.55° to 0.61° after ~4% strain (Fig. 5d). It suggests that ferrite contributes more to uniform deformation through the distribution of strain compared to martensite in both FQP and MQP cases.